Monthly Notices
of the
ROYAL ASTRONOMICAL SOCIETY

MNRAS **473,** 5275–5285 (2018)
Advance Access publication 2017 October 23

doi:10.1093/mnras/stx2709

Predicted stellar kinematics of a kiloparsec-scale nuclear disc (or ring) in the Milky Way

Victor P. Debattista,[1]★ Samuel W. F. Earp,[1] Melissa Ness[2] and Oscar A. Gonzalez[3]

[1] *Jeremiah Horrocks Institute, University of Central Lancashire, Preston, PR1 2HE, UK*
[2] *Max Planck Institut für Astronomie, Königstuhl 17, D-69117 Heidelberg, Germany*
[3] *UK Astronomy Technology Centre, Royal Observatory, Blackford Hill, Edinburgh, EH9 3HJ, UK*

Accepted 2017 October 15. Received 2017 September 15; in original form 2017 March 17

ABSTRACT

In Debattista et al. (2015), we proposed that a kiloparsec-scale nuclear disc is responsible for the high-velocity secondary peak in the stellar line-of-sight velocity distributions (LOSVDs) seen at positive longitudes in the bulge by the Apache Point Observatory Galactic Evolution Experiment (APOGEE). Here, we make further qualitative but distinctive predictions of the kinematic properties of a nuclear disc, including for the LOSVDs at negative longitudes (which APOGEE-2 will observe) and examine the proper motions throughout the disc. Since a nuclear ring is also able to produce similar high-velocity LOSVD peaks, we present predictions for the proper motion signatures which distinguish between a nuclear disc and a nuclear ring. We also demonstrate that the stars in a nuclear disc, which would be on x2 orbits perpendicular to the bar, can remain on these orbits for a long time and can therefore be old. We show that such (old) nuclear discs of comparable size exist in external galaxies.

Key words: Galaxy: bulge – Galaxy: centre – Galaxy: disc – Galaxy: evolution – Galaxy: kinematics and dynamics – Galaxy: structure.

1 INTRODUCTION

Using Apache Point Observatory Galactic Evolution Experiment (APOGEE; Alam et al. 2015) commissioning data, Nidever et al. (2012) studied the line-of-sight velocity distributions (LOSVDs) of stars within the central regions of the Milky Way (MW). They found a secondary (high) peak in Galactocentric velocity (at $V_{\rm GSR} \approx 200\,{\rm km\,s^{-1}}$) for fields in and near the plane, which they proposed is composed of stars on bar orbits. However, the pure N-body models of Li et al. (2014) lack such cool, high-$V_{\rm GSR}$ peaks. Li et al. (2014) also noted a lack of corresponding peaks at the opposite longitudes in the Bulge Radial Velocity Assay (BRAVA; Kunder et al. 2012) data. Their MW N-body model instead showed that the LOSVDs have shoulders extending to large velocities coming from stars at large distance from the Sun. Gómez et al. (2016) find a similar result, also using pure N-body simulations; they fit two Gaussians to the LOSVDs and find that a cool high-velocity component is needed, but that these do not produce the trough observed in the LOSVD. Using the simulation of Li et al. (2014), Molloy et al. (2015) showed that resonant orbits produced high-$V_{\rm GSR}$ peaks. Aumer & Schönrich (2015, hereafter AS15) argued that young stars recently trapped by the bar into resonant orbits are favoured by the selection function of the APOGEE survey. Based on N-body simulations, they proposed that it is preferentially young stars that give rise to the high-$V_{\rm GSR}$ peaks. However, Zasowski et al. (2016) and Zhou et al. (2017) recently showed that stars in the APOGEE high-$V_{\rm GSR}$ peaks do not exhibit distinct chemical abundances or ages, indicating that they are not predominantly comprised of younger stars. As there is no reason for the bar to have stopped growing in the past few gigayears, other models for the high-$V_{\rm GSR}$ peaks need to be considered.

Based on comparison with an N-body+smooth particle hydrodynamics (SPH) simulation with gas and star formation, Debattista et al. (2015, hereafter D15) proposed that the high-$V_{\rm GSR}$ peaks in the mid-plane at $l = 6^\circ$–8° reveal the presence of a kiloparsec-scale nuclear disc, supported by x2 orbits aligned perpendicular to the bar. In their simulation, the nuclear disc forms when gas is driven to the centre by the bar and forms stars. Schönrich, Aumer & Sale (2015) argued that a kiloparsec (kpc) scale is too large a disc for the MW if it forms out of gas reaching the centre now, showing instead that a nuclear disc of 150 pc size is present at the centre of the MW. The presence of a 150 pc-sized nuclear disc in the MW is unsurprising, given that gas now being funnelled by the bar settles into a ring of about this radius (Binney et al. 1991; Weiner & Sellwood 1999; Sormani, Binney & Magorrian 2015; Li et al. 2016). However, Cole et al. (2014) showed that nuclear discs of size comparable to that in the model of D15 exist in early-type galaxies. Moreover, such nuclear discs can be comprised of old stars (e.g. Gadotti et al. 2015), alleviating the problem of needing young stars in the high-$V_{\rm GSR}$ peak.

In order to help test whether a kpc-sized nuclear disc or ring exists in the MW, here we present several predictions for the resulting

★ E-mail: vpdebattista@gmail.com

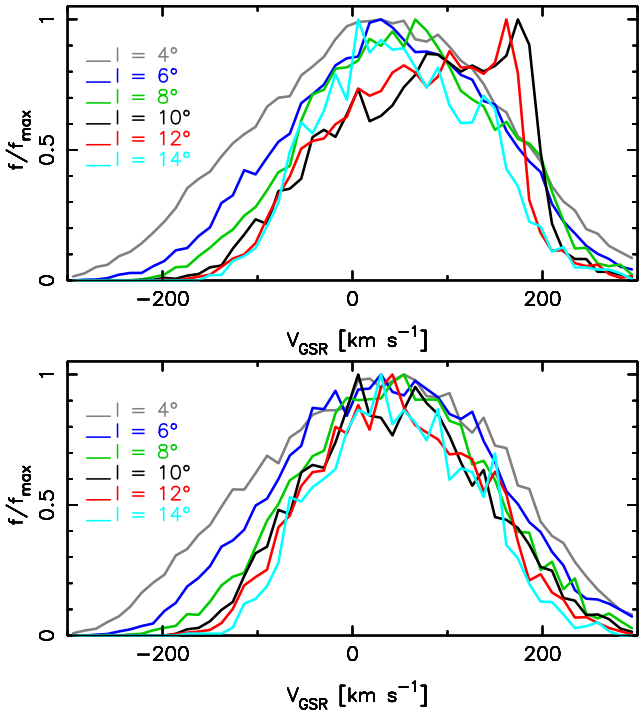

Figure 1. LOSVDs in the model of D15 evolved for a further 6 Gyr with no star formation. Top: in the midplane ($b = 0°$). Bottom: at $b = 2°$. Compare with the right columns of Fig. 1 of D15.

kinematics, which ongoing (e.g. APOGEE-2) and future (e.g. MOONS) surveys can test. We use the same simulation as in D15, observed in the same way, to predict properties of the kinematics that are characteristic of a nuclear disc, particularly at the negative longitudes that have not yet been probed by large surveys. APOGEE-2, in particular, will, in the next few years, measure velocities for bulge stars across negative longitudes, including in the plane. This will provide a homogeneous set of high-resolution spectroscopic data for about 50 000 stars towards the bulge and inner disc across negative and positive longitudes and latitudes (Majewski et al. 2016). We show that the model provides several clear kinematic diagnostics of a nuclear disc or ring from such data.

2 HIGH VELOCITY PEAKS FROM OLD STARS ON X2 ORBITS

D15 showed that a nuclear disc formed in their simulation after 6 Gyr and was well developed by 7.5 Gyr, at which point they used their model to present the LOSVD signatures of a nuclear disc. Because the nuclear disc formed late in their simulation, of necessity the nuclear disc they presented was young. Here, we explore whether the nuclear disc *must* be a young structure, or whether it survives as an old structure. In order to test this, we evolve the model of D15 from 7.5–13.5 Gyr with gas cooling and star formation turned off. During this evolution, the bar roughly doubles in size and the pattern speed drops to 30 per cent of its value at $t = 7.5$ Gyr. At that point, we repeat the same analysis shown in Fig. 1 of D15, presenting the LOSVDs in the midplane and at $b = 2°$. We scale the model exactly as in D15, in order to be able to compare directly with that earlier work.

The LOSVDs in the same lines of sight as in D15 are shown in Fig. 1. In spite of the strong evolution of the bar, high velocity peaks are still evident in the midplane (top panel) at $l = \pm 10°$ and

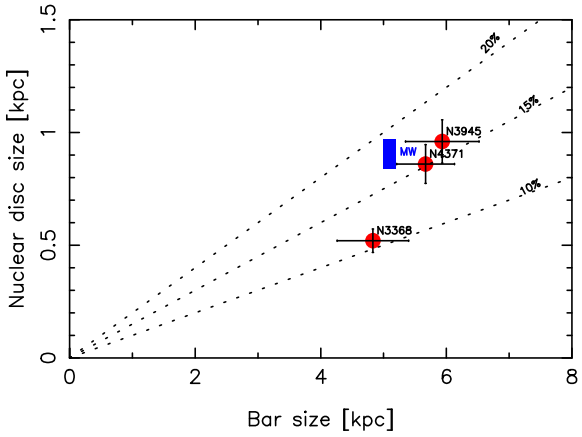

Figure 2. Comparison of the size of the proposed nuclear disc and bar semimajor axes for the MW (blue rectangle, with sides indicating the respective uncertainties) and the sample of galaxies presented by Cole et al. (2014) which all host perpendicular nuclear structures (red circles). Dotted lines indicate constant fraction of bar size, as indicated. The bar size for the MW is from Wegg et al. (2015).

$l = \pm 12°$, although the peak at $l = \pm 8°$ has disappeared. Just as remarkably, the model still retains no signature of a high velocity peak at $b = 2°$ (bottom panel). We will explore the evolution of the peaks in more detail using an orbital analysis elsewhere (Earp et al., in progress).

2.1 Comparison with external galaxies

In D15, we estimated that the nuclear disc needed to explain the high-V_{GSR} peaks in the MW would have a semimajor axis of order 1 kpc. Here, we refine this estimate. Using APOGEE Data Release 12, D15 found tentative evidence of a high velocity peak at $l = 8°$; in Data Release 13, Zhou et al. (2017) find no evidence of a high-V_{GSR} peak in this field. Therefore, we can now assume that the line of sight at $l = 6°$ is tangent to the nuclear disc/ring. We further assume that the nuclear disc/ring has an ellipticity in the range $0 \leq e \leq 0.2$. For a bar angle of 27° to the line of sight (Wegg & Gerhard 2013) and a nuclear structure orthogonal to the bar, we obtain a size 0.84–0.97 kpc, assuming a distance to the Galactic Centre of 8 kpc. In Fig. 2, we compare this size to the nuclear structures observed in three galaxies in which the bar is observed almost perpendicular to the line of nodes, which is the optimal orientation for detecting a nuclear disc/ring orthogonal to the bar. The proposed nuclear disc/ring is similar in size, as a fraction of its bar size, to these galaxies and is therefore not unreasonably large. Moreover, one of the galaxies in this sample, NGC 4371, has a known nuclear disc age of ∼11 Gyr (Gadotti et al. 2015), further demonstrating that such structures built from x2 orbits are stable over long periods.

Therefore, unlike the model of AS15, the high-velocity peaks produced by x2 orbits do not require the presence of preferentially young stars. Since APOGEE has not found young stars in the high velocity peaks (Zasowski et al. 2016; Zhou et al. 2017), this makes the x2 model a very promising model for explaining these peaks in the MW.

3 THE SIMULATION

The simulation we use here is the same one we used in D15, which was described more fully in Cole et al. (2014). Cole et al. (2014) found that a nuclear disc formed in this simulation, which they

showed is qualitatively similar to the nuclear discs in three early-type galaxies. Ness et al. (2014) also studied the same model to compare the stellar age distribution in the bulge with that of the MW. Lastly, Debattista et al. (2017) analysed this model in some detail to demonstrate that all the trends seen in the MW's bulge can be understood as arising from internal evolution via the process of *kinematic fractionation*. We therefore only provide a brief description of the simulation here, and refer to those papers for further details.

The simulation was evolved with the *N*-body+smooth particle hydrodynamics code GASOLINE (Wadsley, Stadel & Quinn 2004). It starts with 5 million gas particles and 5 million dark matter particles. This high mass resolution allows us to use a softening of 100 pc for the dark matter particles and 50 pc for the gas and stellar particles. In the simulation, gas from a hot corona in pressure equilibrium with a dark matter halo cools and settles into a disc. At high gas density (greater than 100 amu cm^{-3}) star formation is triggered; thereafter feedback from star particles is provided via asymptotic giant branch star winds and Types Ia and II supernovae. We use the blastwave prescription of Stinson et al. (2006) to model the supernovae feedback. The gas particles initially all have a mass of $2.7 \times 10^4\,M_\odot$ and stars are born with 35 per cent of this mass. Once the mass of gas particles drops below 21 per cent of their starting value, they are removed and their mass is distributed to the nearest neighbours. By 10Gyr the simulation has formed $\sim 1.1 \times 10^7$ star particles with a total mass of $6.5 \times 10^{10}\,M_\odot$.

3.1 Model scaling and sampling

We adopt the same scaling of the model as in D15 to facilitate comparison with that work. Cole et al. (2014) showed that, after 6 Gyr, the model forms a prominent nuclear disc encircled by an elliptical star-forming ring. By 10Gyr the nuclear disc has a semimajor axis of 1.5kpc and is quite massive and unlikely to match any nuclear disc in the MW. Therefore, we consider the model at 7.5 Gyr (referred to as t_2 in D15) when a strong nuclear disc is established.

The model is more compact and rotates more rapidly than the MW; as in D15, we therefore rescale it in size and velocity. The bar has a size of $\sim$2.1 kpc; assuming the MW's bar is 3.5 kpc long (Gerhard 2002) D15 rescaled all coordinates by a factor of 1.67. D15 rescaled the velocities using a least-squares match of the line-of-sight velocity dispersion of the model to ARGOS survey data (Ness et al. 2013) for all stars within Galactocentric radius $R_{GC} < 3.5$ kpc at $b = 5^\circ$, 7.5° and 10° across $|l| < 15^\circ$. This gives a scaling factor of 0.48 for velocities. While position and velocity scalings lead to the model becoming somewhat similar to the MW, it remains a not very good match to the MW.

We place the observer at $y = -8$ kpc, and orient the bar at 27° to the line of sight (Wegg & Gerhard 2013). We adopt a selection function for star particles in the model:

$$P(R_s) = \begin{cases} w(A) & \text{for2 kpc} \le R_s \le 10\,\text{kpc}, \\ 0 & \text{otherwise}, \end{cases} \quad (1)$$

where R_s is distance from the Sun and $w(A)$ is an age-dependant weight. In most cases, we set $w(A) = 1$ for all ages, as in D15. But we also consider cases where we reduce the weight of just the younger stars, setting $w(A) = 0.1$ or $w(A) = 0.2$ for stars younger than 1 Gyr, to compensate for the high star formation rate. D15 presented examples of LOSVDs with $w(A) = 0.2$ for stars younger than 1 Gyr, which stars in the nuclear disc are. As in D15, when considering distributions of kinematic observables we use an opening angle of 0.5° which matches the smallest size of the APOGEE fields.

3.2 Limitations of the model

The model is useful for interpreting and predicting trends in future data, but it should not be construed as a detailed model of the MW, even after it is rescaled. Its primary advantage is that it is one of the first simulations with gas and star formation where all the stars are formed from gas and where a nuclear disc forms. On the other hand, it has a number of limitations which should give pause to any efforts to test the model on a detailed quantitative basis.

Foremost of the limitations is that the resolution used for the gas is still too large to properly resolve the gas ring size. Sormani et al. (2015) show, using two-dimensional grid calculations with a fixed bar potential, that the size of the gas ring that forms is dependent on the grid cell size, varying by a factor of $\sim$2 when this cell size is changed from 40 to 10 pc (see also Li, Shen & Kim 2015). They interpret this variation as resulting from the need to resolve the cusped x1 orbit, at which point the gas shocks and falls inwards on to x2 orbits (Binney et al. 1991; Sormani et al. 2015). This is primarily a hydrodynamical problem, not one of force resolution. The finite number of particles needed for the SPH kernel results in the gas shocking and transitioning from x1 to x2 orbits at too large a radius, as described by Sormani et al. (2015). Thus, there is every reason to believe that the ring in our simulation, and therefore the nuclear disc that forms from it, is too large, as was already noted by Cole et al. (2014). While the gas disc is too large, this does not mean that the extent of the x2 orbits that support the stellar nuclear disc is too large. The extent of the x2 orbits is set by the gravitational potential which is well resolved on the scale of the stellar disc (corresponding to 20 gravitational softening lengths). It is only how far out on the x2 orbits that the gas settles on to that is at question. Li et al. (2015) show that the extent of x2 orbits is considerably larger than the region where gas settles. Our simulation populates x2 orbits because of still too low mass resolution, but in the MW x2 orbits may have been populated in other ways. For instance, it is possible that external perturbations may give rise to gas settling on such orbits and forming stars.

One of the consequences of the large nuclear disc is that we need to scale the model to an old bar size for the MW, 3.5 kpc. Scaling to Wegg, Gerhard & Portail (2015)'s bar size (5 kpc) results in too large a nuclear disc. This does not imply that the nuclear disc in the MW favours the smaller bar size; indeed our scaling results in a nuclear disc that is still too large to match the MW, with V_{GSR} peaks at slightly larger longitudes than in the MW (D15).

Another issue that arises is that the star formation rate (SFR) in the simulation's nuclear disc is very high. Cole et al. (2014) estimate a SFR of $\sim 1.5\,M_\odot\,yr^{-1}$ within 1 kpc. The MW's Central Molecular Zone is forming stars at a rate of $\sim 0.14\,M_\odot\,yr^{-1}$ (Wardle & Yusef-Zadeh 2008). As a result, the model rapidly builds up to a mass much higher than D15 estimated for a MW nuclear disc. Because of this difference, the stellar nuclear disc is much more prominent in the model's LOSVDs than the high-V_{GSR} peaks in the APOGEE data. D15 present an example of artificially reducing the contribution of young stars by a factor of 5. The resulting LOSVD high-V_{GSR} peak is more realistic relative to the main, low-V_{GSR} peak. Below, we therefore also show the results of reducing these weights, by setting $w(A) = 0.1 - 0.2$.[1]

[1] However, this factor of 10 difference is only with the *current* star formation rate of the MW. We argue that a MW nuclear disc/ring may be quite old, and the MW's star formation rate a earlier times was probably higher. A factor of 10 is therefore probably an overestimate of the amount by which young, nuclear disc stars need to be downweighted for a more realistic comparison with the MW.

Thus, the model is not a good match to the MW. Therefore our predictions from the model are qualitative trends rather than exact kinematic values or locations of features.

4 SIGNATURES OF A NUCLEAR DISC

4.1 Density distribution

Cole et al. (2014) showed that the nuclear disc in the model is elliptical and orientated perpendicular to the main bar, because it is supported by x2 orbits (Earp et al., in progress). Since the near side of the bar in the MW is at positive longitudes, the near side of the nuclear disc is at negative longitudes. Thus, it should be detectable at larger longitudes at $l < 0^\circ$ compared with $l > 0^\circ$. However, because the nuclear disc is rounder than the bar, with ellipticity $\sim$0.2 in the simulation, and because the nuclear disc is almost side-on, the density difference between positive and negative longitudes is small and would be hard to detect.

4.2 Proper motions

We turn therefore to the kinematics to search for evidence of an elliptical nuclear disc. Cole et al. (2014) showed that the kinematics of stars in the bar and in the nuclear disc, which they separated by means of an age cut, are different. Stars in the bar stream along the bar. As seen from the centre of the galaxy, these stars have negative (infalling) radial motions on the leading edge of the bar; nuclear disc stars instead have negative radial motions on the trailing side of the bar. This pattern is produced because the nuclear x2 disc is elongated perpendicular to the bar.

We consider two components of stellar motions as seen from the Sun: $V_{\rm GSR}$, the Galactocentric radial velocity and μ_l, the proper motion in the l direction in the Galactic rest frame. The nuclear disc manifests as an overdensity of stars with low μ_b, the proper motion in the b direction, as is expected for a thin disc. However, the parallax differences between the positive and negative longitude sides of a nuclear disc would be too small to be detectable, rendering vertical proper motions of relatively limited use for understanding the structure of a nuclear disc. We therefore consider the signature of a nuclear disc only in the space spanned by $V_{\rm GSR}$ and μ_l. This space also allows easy interpretation of the LOSVDs that we present in the next section. Fig. 3 presents maps of $\langle V_{\rm GSR}\rangle$ and $\langle\mu_l\rangle$, for predominantly bar stars (top row) and predominantly nuclear disc stars (bottom row), via an age cut. The streaming motions in the nuclear disc are larger overall. In the nuclear disc, $\langle\mu_l\rangle$ is very large and distinct from that of the main bar. Likewise, $\langle V_{\rm GSR}\rangle$ is large to smaller $|l|$ than in the bar stars. These different kinematics as seen from the Sun allow a nuclear disc to be recognized.

Fig. 4 shows the distribution of stars in the model's μ_l–$V_{\rm GSR}$ plane at $b = 0^\circ$ across $-14^\circ \leq l \leq 14^\circ$. The nuclear disc is evident as a narrow, continuous distribution at $|l| \lesssim 10^\circ$ surrounded by a sea of bar and disc particles which produce the large spreads in $V_{\rm GSR}$ and μ_l. As shown by D15, the high-$V_{\rm GSR}$ peaks are absent at $|b| = 2^\circ$ and above, and we also find no sign of the nuclear disc in the μ_l–$V_{\rm GSR}$ plane at this latitude. Any high velocity peaks observed in this region (e.g. Nidever et al. 2012; Zhou et al. 2017) must therefore have an origin other than a nuclear disc.

Fig. 5 deconstructs the trace of the model's nuclear disc in the μ_l–$V_{\rm GSR}$ plane as a function of $R_{\rm s}$. The near side ($R_{\rm s} < 8$ kpc) contributes the $\mu_l > 0$ part of the track, with the distant side providing the negative μ_l part. The near side ($R_{\rm s} < 8$ kpc) of the nuclear disc is at $\mu_l > 0$, which results in the largest absolute proper motions being positive.

A nuclear disc can be seen to be non-axisymmetric in two ways in the μ_l-$V_{\rm GSR}$ plane. First, its track is not symmetric about $V_{\rm GSR} = 0$ when comparing positive and negative l, indicating that the nuclear disc is neither circular nor perpendicular to the line of sight. The nuclear disc also can be seen to not be circular from just a single l. The nuclear disc's track reaches $\mu_l = 0$ at the radius where stars are moving radially towards or away from the Sun. If the nuclear disc were circular, at $\mu_l = 0$ the line of sight would be at the smallest Galactocentric radius within the nuclear disc; the slope of the track would therefore be flat. The clear slope at $\mu_l = 0$ is therefore a sign that a nuclear disc is not axisymmetric. The slope $\mathrm{d}V_{\rm GSR}/\mathrm{d}\mu_l$ is positive because of the orientation of the bar, which places the far side of the nuclear disc at positive l; if the bar angle to the line of sight had been negative, then the slope would be negative.

The nuclear disc in our model is relatively massive, which means that its trace in the μ_l–$V_{\rm GSR}$ plane is clearer than would be the case in the MW. In order to test the significance of the nuclear disc trace at a more realistic mass level, in Fig. 6 we adopt $w(A) = 0.1$ for stars younger than 1 Gyr. The nuclear disc trace is harder to distinguish in large parts of the space, but remains evident at $l = \pm 8^\circ$ and $\pm 10^\circ$.

4.3 Line-of-sight velocity distributions

While proper motions in even a single line of sight crossing a nuclear disc provide considerable diagnostic information, they are still challenging to measure observationally, so we now turn to the LOSVDs. LOSVDs are projections on to the $V_{\rm GSR}$ axis of Fig. 4. These projections often obscure the nuclear disc except in a few select directions. D15 compared the model to APOGEE data at $l > 0^\circ$ and showed some of the signatures by which a nuclear disc can be recognized. A nuclear disc is evident in LOSVDs at positive longitudes as a high-$V_{\rm GSR}$ peak, which is cooler (narrower) than the dominant low-$V_{\rm GSR}$ peak, and is absent off the midplane. Moreover, the distribution around the high-$V_{\rm GSR}$ peak is skewed towards smaller $V_{\rm GSR}$. D15 found that the first three properties are matched by the APOGEE LOSVDs at $l = 6^\circ$–8°. However, the signal-to-noise ratio (number of stars observed) was not sufficiently high to make definitive statements about the skewness.

Fig. 7 presents the LOSVDs of the model at negative longitudes. The top panel of Fig. 7 shows the LOSVDs at the opposite longitudes to those in D15 (their Fig. 1). At negative longitudes, we find the same four basic predictions with some differences characteristic of an elliptical nuclear disc. The first obvious difference produced by the ellipticity of a nuclear disc is that the high-$V_{\rm GSR}$ peak extends to larger $|l|$ on the negative side compared with the positive side, because the near side of the nuclear disc is at $l < 0^\circ$.

Fig. 4 showed that a nuclear disc on the near side of the bulge produces a high-$V_{\rm GSR}$ peak at $l > 0^\circ$. Correspondingly, the nuclear disc on the far side of the bulge produces the high-$V_{\rm GSR}$ peaks at $l < 0^\circ$. In general, the peak $|V_{\rm GSR}|$ is larger at $l > 0^\circ$ than at $l < 0^\circ$, because the line of sight crosses the nuclear disc closer to its minor axis, where the velocity is larger. The top panel of Fig. 7 shows that the high-$V_{\rm GSR}$ peak in our model is at $|V_{\rm GSR}| \simeq 180\,\mathrm{km\,s^{-1}}$ at $l < 0^\circ$; in contrast at $l > 0^\circ$ the peak is at $V_{\rm GSR} \simeq 200\,\mathrm{km\,s^{-1}}$. Conversely, because the lines of sight on the $l < 0^\circ$ side intersect the nuclear disc at a smaller range of Galactocentric distances than at $l > 0^\circ$, the $l < 0^\circ$ peak has a narrower range of velocities, i.e. it appears cooler, than at $l > 0^\circ$.

The second panel of Fig. 7 compares the LOSVDs at negative and positive longitudes directly, transforming $V_{\rm GSR}$ to $-V_{\rm GSR}$ for the

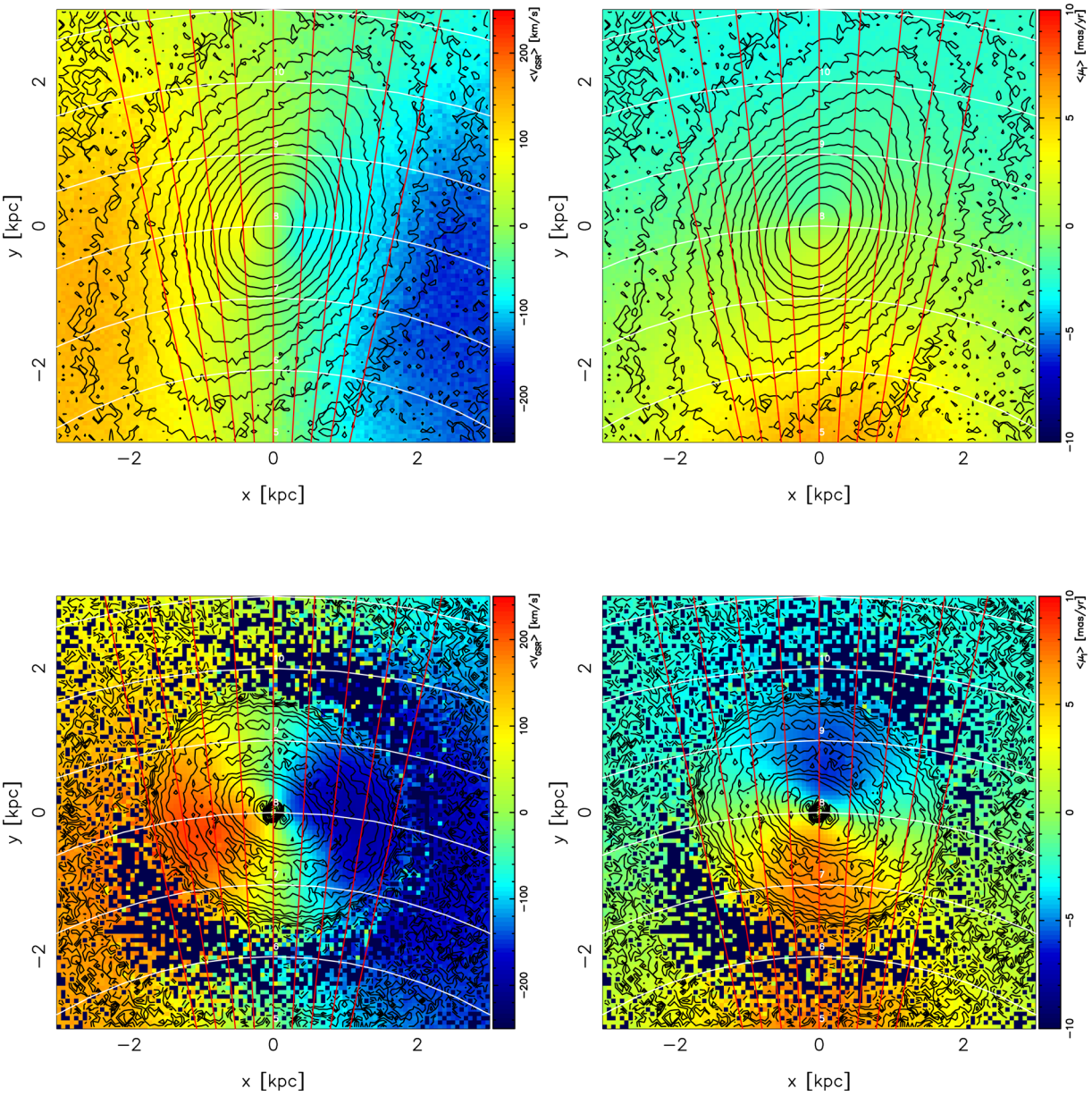

Figure 3. Kinematics of the model for predominantly bar (age >2 Gyr) stars (top row) versus predominantly nuclear disc (age <0.5 Gyr) stars (bottom row) as seen from the Sun (x, $y = 0$, -8 kpc). Left-hand panels show $\langle V_{\rm GSR}\rangle$, while right-hand panels show $\langle \mu_l \rangle$. White circles indicate constant distance from the Sun, $R_{\rm s}$, while red lines show $l = 0°$, $\pm 3°$, $\pm 6°$, $\pm 9°$, and $\pm 12°$.

negative l bins. Aside from the high-$V_{\rm GSR}$ peak occurring at smaller $|V_{\rm GSR}|$ and being cooler, at negative longitudes, two additional geometric effects are evident. In the low-$V_{\rm GSR}$ peak, the LOSVD is higher at $l > 0°$, which occurs because the path length through the bar there is longer and intersects the bar at smaller Galactic radii (Blitz & Spergel 1991). For the same reason, the high-$V_{\rm GSR}$ peak is more pronounced on the $l < 0°$ side. Therefore, a high-$V_{\rm GSR}$ peak is easier to detect at negative longitudes. This asymmetry is a key signature of an elliptical nuclear disc.

The third and fourth row of Fig. 7 are identical to the second row but set $w(A) = 0.1$ and 0.2, respectively, for stars younger than 1 Gyr. Even in the case where $w(A) = 0.1$, which is probably an overestimate of the correction required, high-$V_{\rm GSR}$ peaks are evident, although the peak in the $l = -12°$ bin is ambiguous.

Fig. 8 shows the contribution of stars at different distances from the observer, $R_{\rm s}$, on the LOSVDs at $l = \pm 10°$. The stars in the high-$V_{\rm GSR}$ peak are all at $7 \leq R_{\rm s}/\,{\rm kpc} \leq 9$.

4.4 The signature of a ring

While D15 interpreted the high-$V_{\rm GSR}$ peaks found by AGPOGEE as due to a disc, a nuclear ring supported by x2 orbits is an equally viable interpretation. The fact that the nuclear loci in the μ_l–$V_{\rm GSR}$ plane are continuous shows that the nuclear structure is a disc. While the structure is continuous, a ring surrounds the nuclear disc in our simulation and manifests as the peaks at the ends of the nuclear disc track in the μ_l–$V_{\rm GSR}$ plane. This also shows what the signature of a nuclear *ring* would be: two disconnected overdensities in the μ_l-$V_{\rm GSR}$ plane at most longitudes, merging when the ring is seen

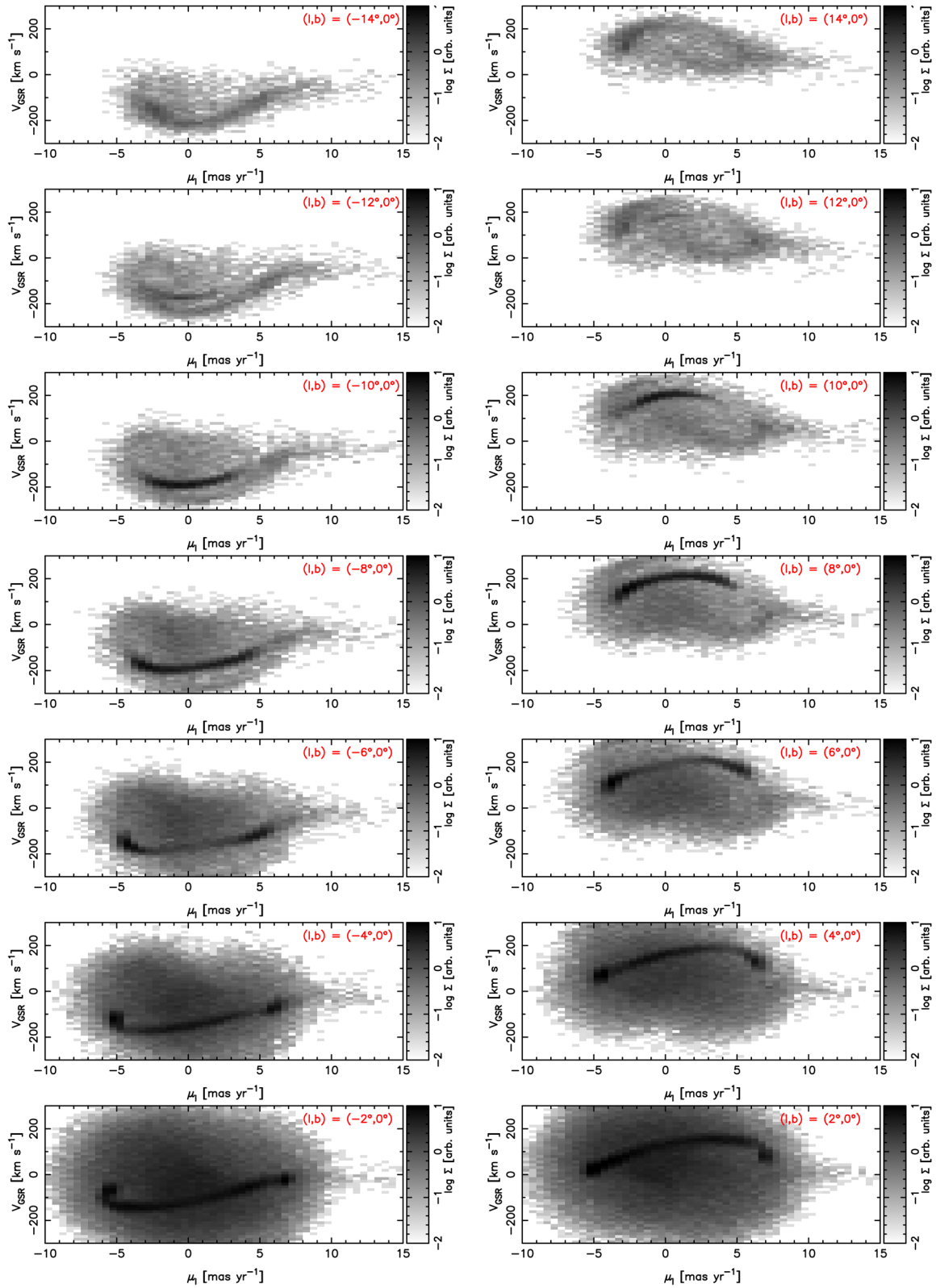

Figure 4. μ_l versus V_{GSR} of the model for different lines of sight in the midplane.

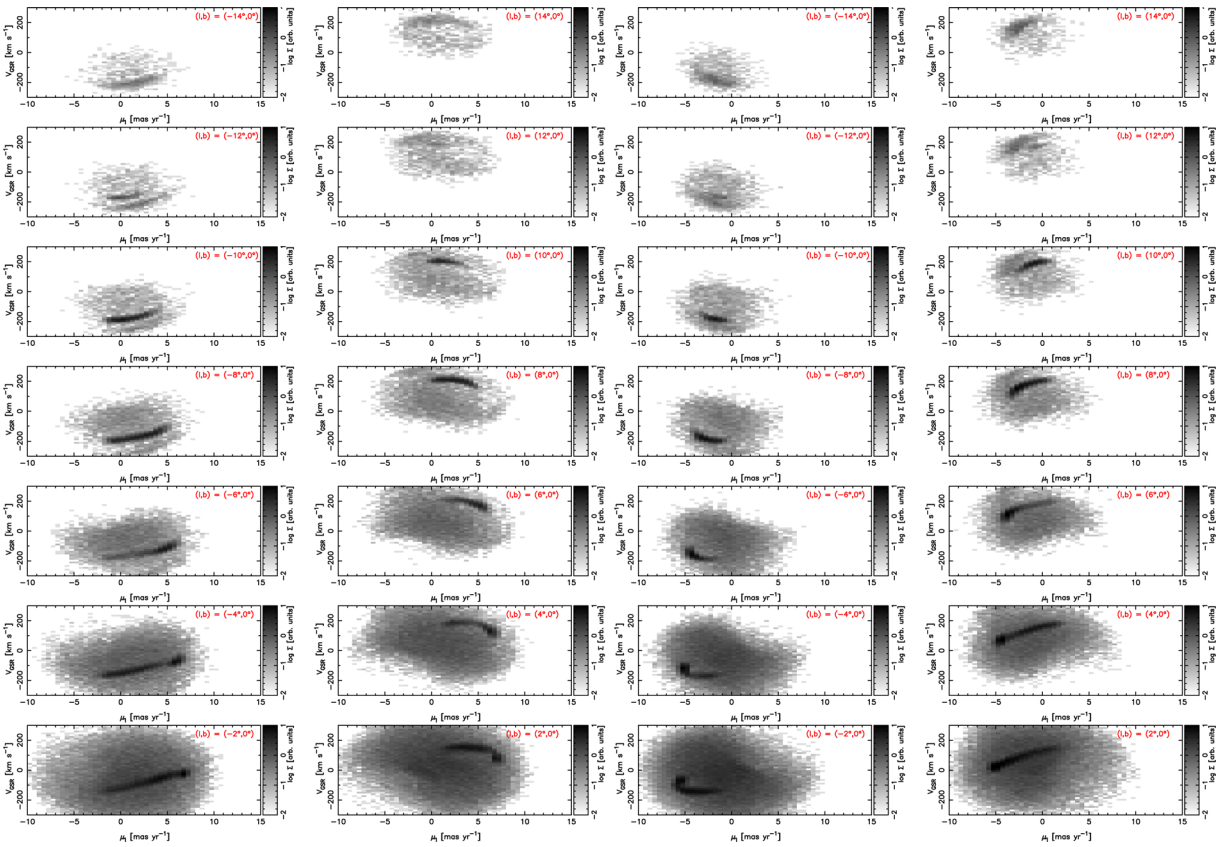

Figure 5. μ_l versus $V_{\rm GSR}$ of the model for different lines of sight in the midplane. Left two columns: near side ($6.5 \leq R_{\rm s}/\,{\rm kpc} \leq 8$) stars. Right two columns: far side ($8 \leq R_{\rm s}/\,{\rm kpc} \leq 9.5$) stars.

tangentially. Fig. 9 shows an example of a nuclear ring, taken from the simulation evolved for 6 Gyr without star formation, discussed in Section 2; the substantial evolution during this time leads to the nuclear disc transforming into a ring. This is clear in the μ_l–$V_{\rm GSR}$ plane as the disconnected pair of density peaks seen at $l = \pm 6^\circ$ and at $l = 8^\circ$. At $l = \pm 10^\circ$ and $l = \pm 12^\circ$ the nuclear ring is seen close to tangentially and the trace in the μ_l–$V_{\rm GSR}$ plane is continuous.

5 DISCUSSION

We have presented further kinematic signatures of a nuclear disc at the centre of the MW, particularly at negative longitudes, which will be surveyed by APOGEE-2 and MOONS. The principal signatures we predicted are as follows:

(i) We showed that the LOSVDs contain second, high-$V_{\rm GSR}$, peaks at $l < 0^\circ$ just as they do at $l > 0^\circ$. The high-$V_{\rm GSR}$ peaks are cooler than the low-$V_{\rm GSR}$ peaks and skewed to smaller $|V_{\rm GSR}|$, just as in the $l > 0^\circ$ case.

(ii) The LOSVDs at positive longitudes peak at larger $|V_{\rm GSR}|$ but the peaks are visible to smaller $|l|$, than at negative longitude. These two properties are a result of the elliptical nature of a nuclear disc and the fact that it would be perpendicular to the bar.

(iii) Moreover the $l < 0^\circ$ high-$V_{\rm GSR}$ peaks are higher than the $l > 0^\circ$ ones. Testing this property is only possible if the selection function is very well understood.

(iv) The proper motion in the latitude direction, μ_b, shows only a narrow distribution, consistent with a population that is thin, which can be inferred already from the absence of high-$V_{\rm GSR}$ peaks off the mid-plane. Any high-$V_{\rm GSR}$ peaks at $|b| \sim 2^\circ$ cannot be explained by a nuclear disc.

(v) In the μ_l–$V_{\rm GSR}$ plane the nuclear disc stands out as a continuous track of enhanced density. The narrowness of the track indicates a relatively low dispersion in the nuclear disc.

(vi) The asymmetry across $l = 0^\circ$ and the non-zero slope $\mathrm{d}V_{\rm GSR}/\mathrm{d}\mu_l$ at $\mu_l = 0\,{\rm mas\,yr^{-1}}$ are both signs that a nuclear disc is not axisymmetric.

(vii) A nuclear ring produces LOSVD peaks very similar to a nuclear disc; whether a nuclear disc or a nuclear ring is present can be determined by whether the track in the μ_l–$V_{\rm GSR}$ plane is continuous or not. Assuming that the high-$V_{\rm GSR}$ peaks observed by APOGEE at $l = 6^\circ$ are the tangent points of a nuclear structure, the ideal location to test whether a ring or a disc is present is at $l = 3^\circ$–4°.

5.1 Distinction with the model of AS15

Our model and the model of AS15 are fundamentally very different so it should be possible to tell them apart; in our model, an old disc or ring of x2 orbits orthogonal to the bar gives rise to the high-$V_{\rm GSR}$ peaks, while in the AS15 model, the high-$V_{\rm GSR}$ stars are predominantly on x1 and higher order orbits, generally elongated parallel to the bar, and which have recently been trapped by the bar. In this model, the high-$V_{\rm GSR}$ stars are preferentially young. However, ages are always difficult to measure unambiguously so we turn to kinematic differences between the models. Because of the very different orientations between the relevant orbits in the two models, clear kinematic differences are expected. The most promising distinction between the two models is a geometric one that comes from comparing the high-$V_{\rm GSR}$ stars at positive and negative longitudes. At positive longitudes, APOGEE finds a statistically

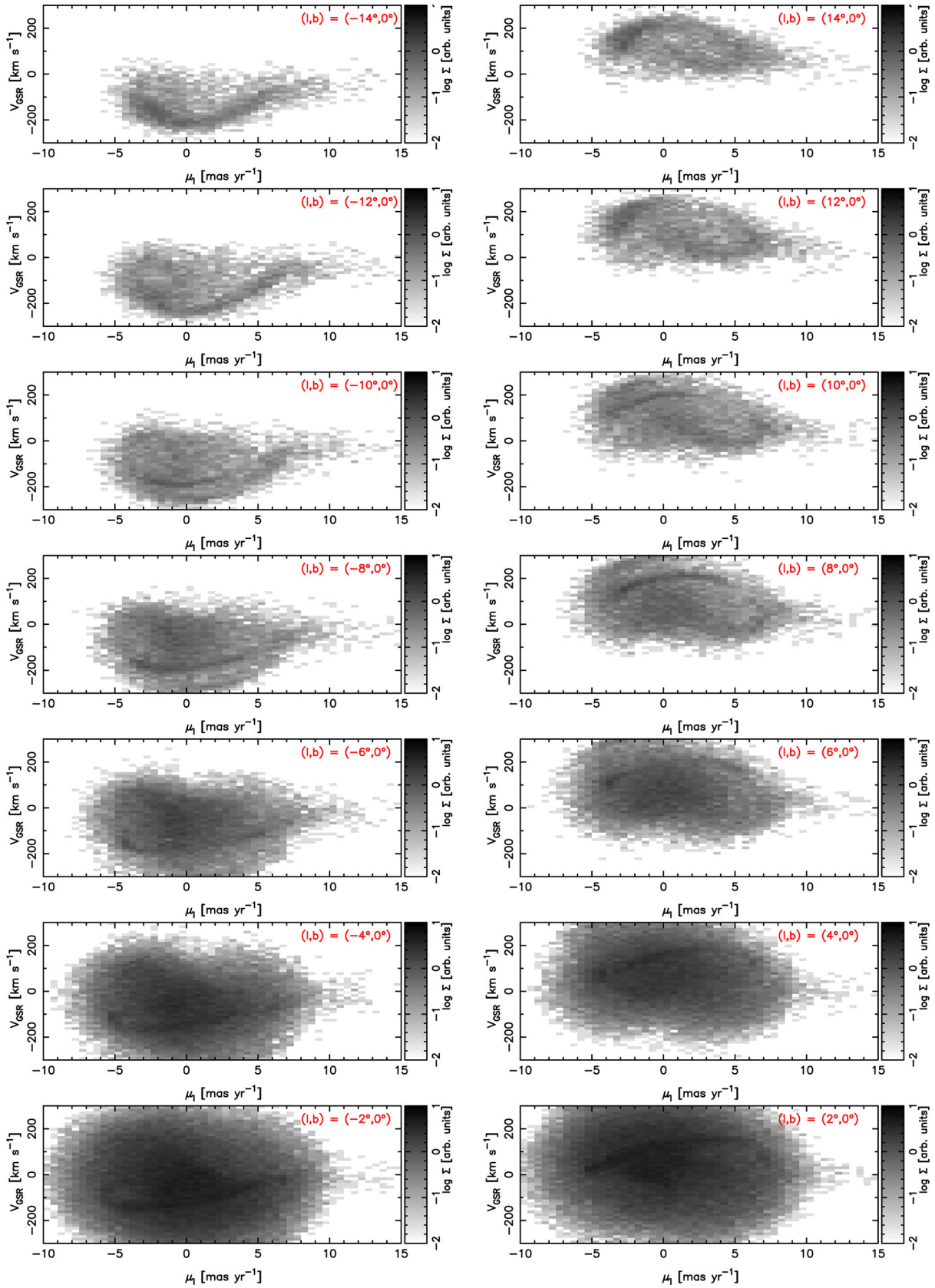

Figure 6. μ_l versus V_{GSR} of the model for different lines of sight in the midplane with $w(A) = 0.1$ for stars younger than 1 Gyr.

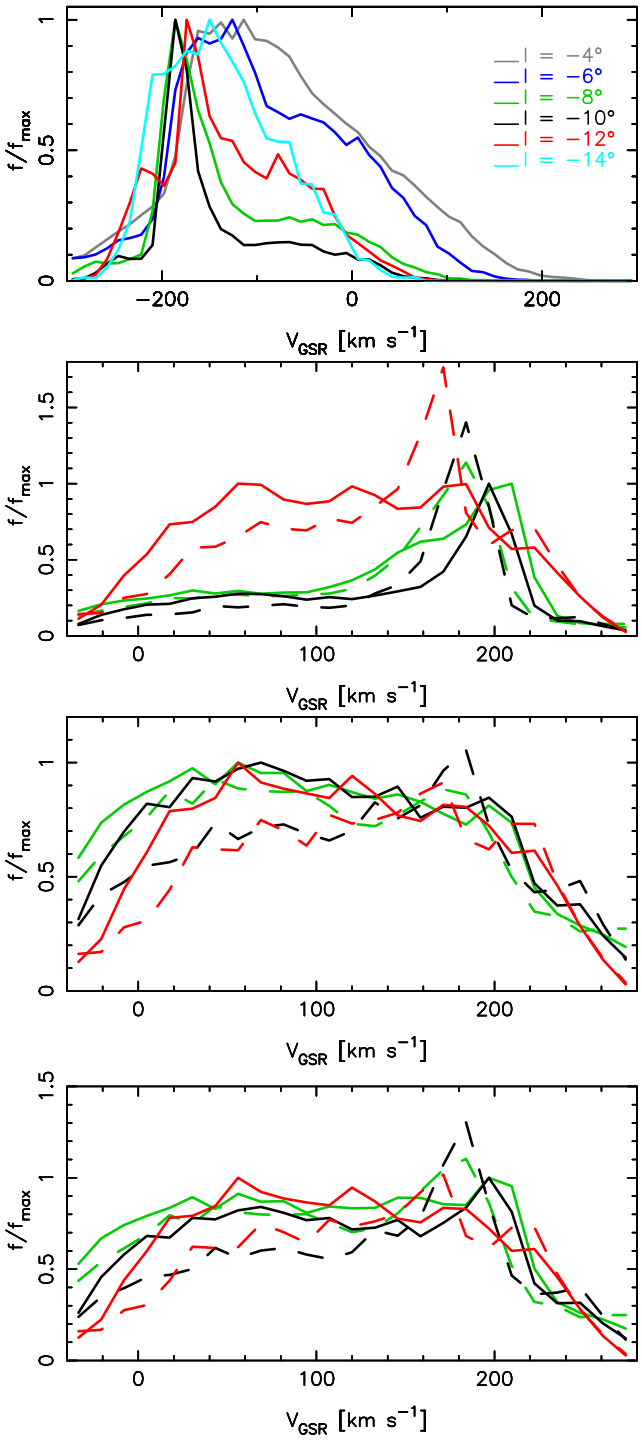

Figure 7. Top: mid-plane LOSVDs for the model at negative longitudes, as indicated. Each LOSVD has been normalized to unit peak. Second row: comparison between the model's midplane LOSVDs at negative and positive longitudes. Solid lines show $l > 0°$ while dashed lines show $l < 0°$ (with the sign of $V_{\rm GSR}$ reversed). At each longitude, the LOSVDs are normalized to the peak at positive l. Colours indicate $|l|$ as in the top panel. Third and fourth rows: identical to second row with $w(A) = 0.1$ and 0.2, respectively.

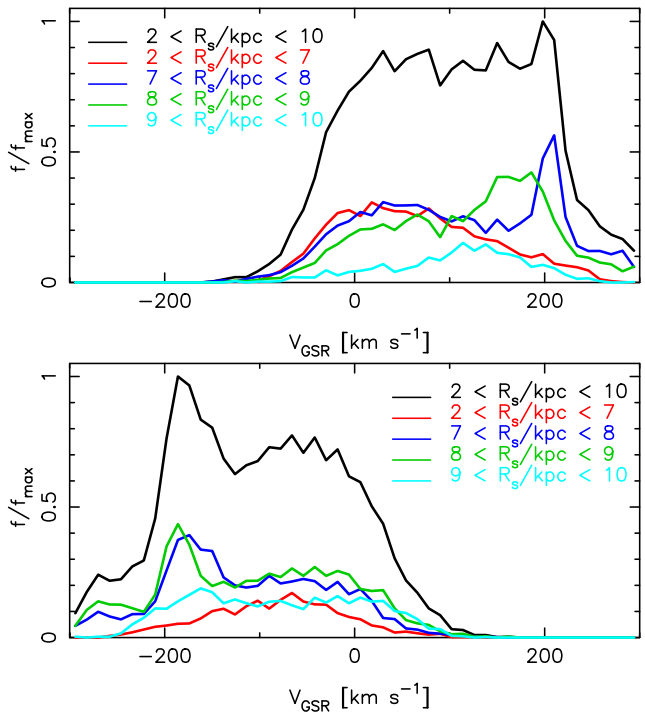

Figure 8. Decomposition by distance from the Sun of the model's LOSVDs in the fields at $l = +8°$ (top) and $l = -8°$ (bottom), with $w(A)$ set to 0.2 for stars younger than 1 Gyr for the sake of clarity. In both panels, the LOSVDs are normalized to the peak of the LOSVD for the full distance ($2 \leq R_{\rm s}/{\rm kpc} \leq 10$) range in that longitude.

significant secondary peak at $(l, b) = (6°, 0°)$ (Zhou et al. 2017) with a velocity ∼220–250 km s^{-1} (D15). The x2 orbit model predicts that at $l = -6°$ the peak velocity will appear at a lower velocity, by ∼20 km s^{-1} than at $l = +6°$. In contrast, the model of AS15 predicts that, in the absence of a dominant young stellar population, a shoulder is present at a larger velocity, ∼250 km s^{-1}. We propose therefore that a very simple test of the two models can be produced by comparing the midplane LOSVDs at $l = 6°$ and $l = -6°$. If the secondary peak is at lower $|V_{\rm GSR}|$ in the $l = -6°$ field then this is evidence in favour of an x2 feature. If instead the feature is at larger $|V_{\rm GSR}|$, then this favours the model of AS15. In the absence of young stars at high-$V_{\rm GSR}$, further evidence in favour of the x2 model can be obtained if improved statistics at the $(l, b) = (+6°, 0°)$ field show that a peak, rather than the shoulder predicted by the AS15 model, is present.

5.2 Conclusions

We have presented predictions for the one-dimensional (LOSVD) and two-dimensional (μ_l–$V_{\rm GSR}$) kinematics of a nuclear stellar ring or disc. Confirmation of such a system, which would be considerably larger than the radius at which gas is now being delivered to the Galactic centre by the bar, would constitute an important clue to the early evolution of the MW's bar. APOGEE-2 will shortly be delivering the LOSVD data at negative longitudes towards the bulge. These data have the potential to confirm or reject the presence of a kiloparsec-scale nuclear x2-orbit structure. Distinguishing whether the structure is a ring or a disc requires proper motions and such measurements of the required precision, while challenging, are already possible (e.g. Calamida et al. 2014). We therefore look forward to a future possibility where the dynamical imprint of the

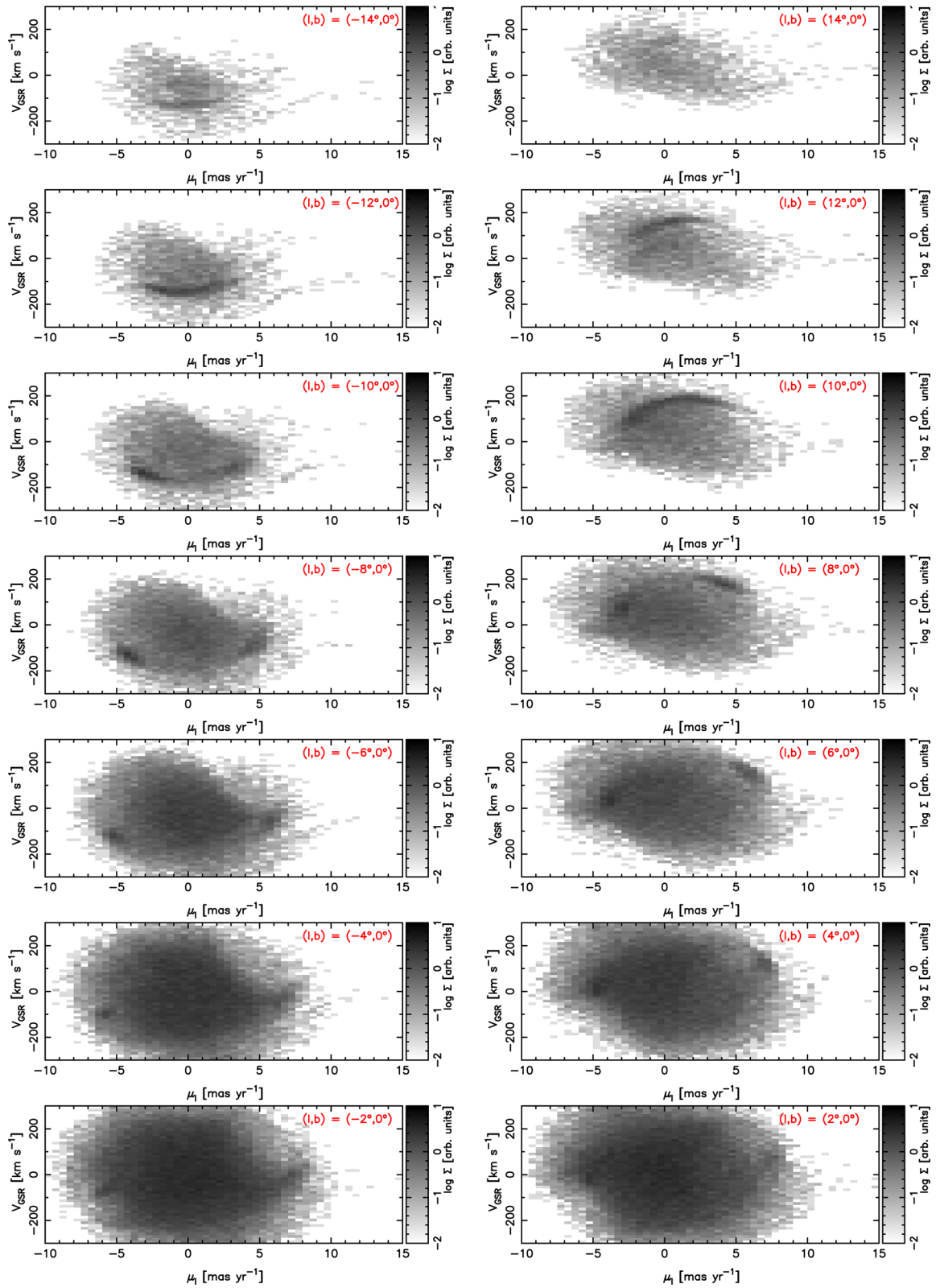

Figure 9. μ_l versus V_{GSR} for different lines of sight in the midplane for the simulation evolved from 7.5 to 13.5 Gyr with gas cooling and star formation turned off.

early evolution of the MW is captured in the fossil evidence at the centre.

ACKNOWLEDGEMENTS

VPD is supported by STFC Consolidated grant # ST/M000877/1. MN acknowledges funding from the European Research Council under the European Union's Seventh Framework Programme (FP 7) ERC Advanced grant agreement no. 321035. The simulation used in this paper was run at the High Performance Computing Facility of the University of Central Lancashire. We thank Ralph Schönrich, Monica Valluri and Juntai Shen for fruitful discussion and Anita Kotla for proofreading the paper.

REFERENCES

Alam S. et al., 2015, ApJS, 219, 12
Aumer M., Schönrich R., 2015, MNRAS, 454, 3166
Binney J., Gerhard O. E., Stark A. A., Bally J., Uchida K. I., 1991, MNRAS, 252, 210
Blitz L., Spergel D. N., 1991, ApJ, 379, 631
Calamida A. et al., 2014, ApJ, 790, 164
Cole D. R., Debattista V. P., Erwin P., Earp S. W. F., Roškar R., 2014, MNRAS, 445, 3352
Debattista V. P., Ness M., Earp S. W. F., Cole D. R., 2015, ApJ, 812, L16
Debattista V. P., Ness M., Gonzalez O. A., Freeman K., Zoccali M., Minniti D., 2017, MNRAS, 469, 1587
Gadotti D. A., Seidel M. K., Sánchez-Blázquez P., Falcón-Barroso J., Husemann B., Coelho P., Pérez I., 2015, A&A, 584, A90
Gerhard O., 2002, in Da Costa G. S., and Helmut Jerjen, eds, ASP Conf. Ser. Vol. 273: The Dynamics, Structure & History of Galaxies: A Workshop in Honour of Professor Ken Freeman. Astron. Soc. Pac., San Francisco, p. 73
Gómez A., Di Matteo P., Stefanovitch N., Haywood M., Combes F., Katz D., Babusiaux C., 2016, A&A, 589, A122
Kunder A. et al., 2012, AJ, 143, 57
Li Z., Shen J., Kim W.-T., 2015, ApJ, 806, 150
Li Z., Gerhard O., Shen J., Portail M., Wegg C., 2016, ApJ, 824, 13
Li Z.-Y., Shen J., Rich R. M., Kunder A., Mao S., 2014, ApJ, 785, L17
Majewski S. R. et al., 2016, Astron. Nachr., 337, 863
Molloy M., Smith M. C., Evans N. W., Shen J., 2015, ApJ, 812, 146
Ness M. et al., 2013, MNRAS, 432, 2092
Ness M., Debattista V. P., Bensby T., Feltzing S., Roškar R., Cole D. R., Johnson J. A., Freeman K., 2014, ApJ, 787, L19
Nidever D. L. et al., 2012, ApJ, 755, L25
Schönrich R., Aumer M., Sale S. E., 2015, ApJ, 812, L21
Sormani M. C., Binney J., Magorrian J., 2015, MNRAS, 449, 2421
Stinson G., Seth A., Katz N., Wadsley J., Governato F., Quinn T., 2006, MNRAS, 373, 1074
Wadsley J. W., Stadel J., Quinn T., 2004, New Astron., 9, 137
Wardle M., Yusef-Zadeh F., 2008, ApJ, 683, L37
Wegg C., Gerhard O., 2013, MNRAS, 435, 1874
Wegg C., Gerhard O., Portail M., 2015, MNRAS, 450, 4050
Weiner B. J., Sellwood J. A., 1999, ApJ, 524, 112
Zasowski G., Ness M. K., García Pérez A. E., Martinez-Valpuesta I., Johnson J. A., Majewski S. R., 2016, ApJ, 832, 132
Zhou Y. et al., 2017, ApJ, 847, 74

This paper has been typeset from a TEX/LATEX file prepared by the author.